ISSN 1392-1207. MECHANIKA. Vol. 30, No. 4, 2024: 357–364

Barrier Lyapunov Based Adaptive Control for Hydraulic Servo Systems with Parametrical Nonlinearities and Modeling Uncertainties

Zhenshuai WAN*, Yu FU, Chong LIU***, Longwang YUE******
**School of Mechanical and Electrical Engineering, Henan University of Technology, Zhengzhou, 450001, China, E-mail: wanzhenshuai@haut.edu.cn (Corresponding author)*
***School of Mechanical and Electrical Engineering, Henan University of Technology, Zhengzhou, 450001, China*
****School of Mechanical and Electrical Engineering, Henan University of Technology, Zhengzhou, 450001, China*
*****School of Mechanical and Electrical Engineering, Henan University of Technology, Zhengzhou, 450001, China*
https://doi.org/10.5755/j02.mech.34528

1. Introduction

Hydraulic servo systems are widely used in industrial fields, such as earthquake simulator, vehicle active suspension, heavy mining equipment in virtue of their high power-to ratios, fast response, large force/torque output and good robustness [1-4]. However, the parametrical nonlinearities including input saturation, dynamic friction and valve overlap hinder the high precision position tracking of hydraulic equipment [5-7]. In addition, the hydraulic system uncertainties (e.g., bulk modulus, load variation, oil leakage, external disturbance) also complicate the controller design [8]. Hence, the traditional linear models cannot meet the requirement of high-performance dynamic response and small steady-state precision for modern industrial process control [9]. More importantly, these nonlinearities and uncertainties may degrade performance and even result in control system unstable [10]. Nevertheless, current hydraulic servo systems demand both transient response performance and tracking precision. To meet this requirement, it is very necessary to enhance the control response performance in hydraulic system.

To retain satisfying tracking performance, numerous control schemes have been developed, such as proportional-integral-derivative (PID) control [11], adaptive control (AC) [12-14], robust control [15-17], backstepping control [18-20], fuzzy control [21] and neural network control [22,23]. Classical PID control may not achieve satisfy tracking performance when there are model uncertainties, parameter fluctuations and external disturbance. To cope with the drawbacks of traditional PID control, intelligent optimization algorithm is integrated with PID to on-line adjust controller's parameters [24]. Yao et.al developed an adaptive controller to deal with parametric uncertainties along with nonlinear friction compensation of hydraulic systems, where adaptive control law and robust control law is designed in backstepping controller to achieve excellent tracking performance [25]. Deng et al utilized robust controller to addresses the high precision position control of hydraulic system with parametric uncertainties and unmodeled disturbances by introducing a nonlinear robust term [26]. Guo et. al proposed backstepping controller to handle unknown load disturbance and uncertain nonlinearity by using extended-state-observer [18]. Shen et. al proposed fuzzy controller to solve the parametric coupling and intrinsic nonlinearity of hydraulic cylinder, where fuzzy system is used to approximate the minimum sliding mode gain [21]. Guo et al presented a neural network–based adaptive composite dynamic surface controller, where neural network is employed to estimate the system state and unknown nonlinearity of dynamic friction [27].

Despite the aforementioned control methods have good tracking performance, they did not take state constraints into consideration. In real world, the practical systems abide the effect of the constraints, such as pressure of hydraulic cylinder and physical limitation of system [28]. Song et al. investigated an adaptive controller f to solve the full-state and input constraints of motors, where log-type barrier Lyapunov function (BLF) is used to deal with output performance constraint, input constraints, and unknown external disturbances [29]. Liu et al used adaptive learning controller to cope with the state constraints of nonlinear systems, where the BLF were designed to guarantee that the state constraints are bounded [30]. The abovementioned control methods can solve the constant constraint problem well to some extent. In this paper, in order to relax the conditions of the system constant constraint, the time-varying asymmetric barrier Lyapunov function (TABLF) is selected the intermediate function in each step of backstepping design. In addition, the adaptive law can also be used to update the disturbance upper bounds online, which improves the operability of the controller in practical applications.

This paper is organized as follows. Problem formulation and dynamic model are described in section 2. In section 3, the controller design is presented and the system stability is analysed. Section 4 proposes comparative simulation results. Some conclusions are provided in section 5.

2. Problem formulation and dynamic model

In this section, the nonlinear dynamic model of the hydraulic servo system is given. Fig.1 shows the considered hydraulic servo system, which mainly contains pump, actuator, servo valve and other components. The hydraulic actuator drives the load to move the desired position. The servo valve determines the direction of the motion and the speed of hydraulic actuator by controlling the spool position. The accumulator installed next to the pump acts as energy replenishment device. The relief valve plays an important role in protecting equipment operation by controlling the maximum of work pressure. The control goal hydraulic servo system is to make the load track the desired signal as closely as possible by adjusting the output pressure of hydraulic cylinder.

The dynamics equation of load is described as follows

$$m\ddot{y} = P_L A - B\dot{y} - Ky + f\left(y,\dot{y},t\right), \tag{1}$$

where m is the displacement of load, y is the mass of load; P_L=P_1-P_2 is the load pressure; A is the efficient ram area; B is the viscous coefficient; f is the unmodeled disturbance.

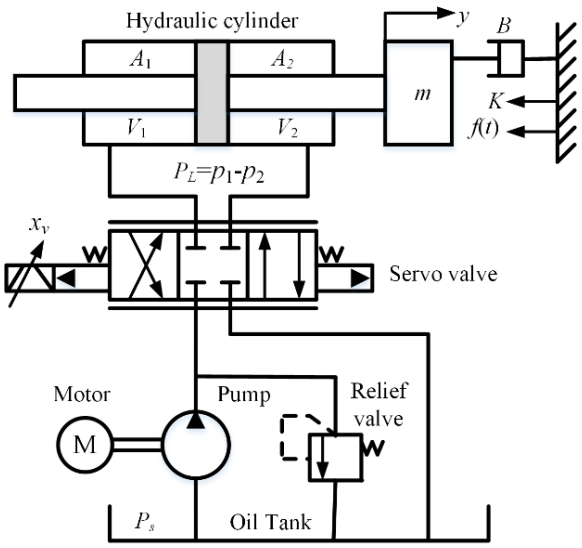

Fig. 1 Control mechanism of hydraulic servo system

The fluid dynamic equation of the actuator is described as

$$\frac{V_t}{4\beta_e}\dot{P}_L = -A\dot{y} - C_t P_L + Q_L, \tag{2}$$

where V_t is the total volume of the actuator; β_e is the effective bulk modulus, C_t is the coefficient of the internal leakage, Q_L=(Q_1+Q_2)/2 is load flowrate, in which Q_1 and Q_2 are the supplied flowrate and return flowrate. The load flowrate Q_L can be described by

$$Q_L = C_d w x_v \sqrt{\frac{P_s - sign(x_v)P_L}{\rho}}, \tag{3}$$

where C_d is the discharge coefficient, w is the spool valve area gradient, x_v is the spool valve displacement, P_s is the supply pressure, ρ is the oil density. The sign function is given by

$$sign(*) = \begin{cases} 1 & \text{if} * > 0 \\ 0 & \text{if} * = 0 \\ -1 & \text{if} * < 0 \end{cases}. \tag{4}$$

The relationship between spool position x_v and servo valve control input voltage u can be described as x_v=$k_i u$, where k_i is a positive electrical constant. Therefore, Eq. (3) can be rewritten as

$$Q_L = ku\sqrt{P_s - \text{sign}\left(x_v\right)P_L}, \tag{5}$$

where $k = C_d w k_i \sqrt{1/\rho}$.

Define $x = [x_1, x_2, x_3]^T = [y, \dot{y}, P_L]^T$, combining Eqs. (1)-(5), the system state space can be described as

$$\begin{cases} \dot{x}_1 = x_2 \\ \dot{x}_2 = \dfrac{1}{m}(-Kx_1 - Bx_2 + Ax_3 + f) \\ \dot{x}_3 = -\dfrac{4A\beta_e}{V_t}x_2 - \dfrac{4\beta_e C_t}{V_t}x_3 + \\ \quad + \dfrac{4\beta_e k}{V_t}\sqrt{P_s - sign(x_v)x_3}u \end{cases}. \tag{6}$$

Remark 1. The hydraulic parameters C_d, ρ, K, B, β_e, C_t are always uncertain positive constants.

Remark 2. The unmodeled disturbance f is bounded by $|f| \leqslant f_{\max}$., where $f_{\max}$ is a positive constant.

Based on remarks 1and 2, the dynamical model of hydraulic servo system (6) is written as

$$\begin{cases} \dot{x}_1 = x_2 \\ \dot{x}_2 = f_2\left(\bar{x}_2\right) + g_2\left(\bar{x}_2\right)x_3 \\ \dot{x}_3 = f_3\left(\bar{x}_3\right) + g_3\left(\bar{x}_3\right)u \end{cases}, \tag{7}$$

where four model function are designed as

$$\begin{cases} f_2\left(\bar{x}_2\right) = -\dfrac{Kx_1 + Bx_2}{m} \\ g_2\left(\bar{x}_2\right) = \dfrac{A + f}{m} \\ f_3\left(\bar{x}_3\right) = -\dfrac{4A\beta_e}{V_t}x_2 - \dfrac{4\beta_e C_t}{V_t}x_3 \\ g_3\left(\bar{x}_3\right) = \dfrac{4\beta_e k}{V_t}\sqrt{P_s - sign\left(x_v\right)x_3}u \end{cases}. \tag{8}$$

3. Controller design

The nonlinearities and modeling uncertainties of hydraulic servo system is given by

$$f_i(x_i) = \varphi_i(x_i)\theta^T, \tag{9}$$

where $\varphi_i(x_i)$, θ are known function and unknown vector, respectively. In addition, $\hat{\theta}$ is the estimation of θ and $\tilde{\theta} = \hat{\theta} - \theta$.

Define $z_1 = x_1 - y_d$ and $z_i = x_i - \alpha_{i-1}$, i = 2, 3, where α_{i-1} is a virtual law which is designed in backstepping controller. For the sake of narrative, the definition is first introduced.

$$\begin{cases} q_i(z_i) = 1 & z_i > 0 \\ q_i(z_i) = 0 & z_i \leq 0 \end{cases}, \tag{10}$$

$$\begin{cases} \xi_{a_i}(t) = \dfrac{z_i}{k_{a_i}(t)}, \xi_{b_i}(t) = \dfrac{z_i}{k_{b_i}(t)} \\ \xi_i = q_i(z_i)\xi_{b_i}(t) + (1 - q_i(z_i))\xi_{a_i}(t) \end{cases}, \tag{11}$$

$$u_i = \frac{q_i(z_i)}{k_{b_i}^{2p} - z_i^{2p}} + \frac{1-q_i(z_i)}{k_{a_i}^{2p} - z_i^{2p}}, \quad (12)$$

$$k_i^u(t) = \sqrt{(\dot{k}_{b_i}(t)/k_{b_i}(t))^2 + (\dot{k}_{a_i}(t)/k_{a_i}(t))^2 + \beta_i}, \quad (13)$$

where β_i is a positive constant, $-k_{a_i}(t) < z_i(t) < k_{b_i}(t)$, $k_{a_i}(t)$ and $k_{b_i}(t)$ are design parameters.

Step 1: The time derivative of z_1=x_1-y_d is

$$\dot{z}_1 = \dot{x}_1 - \dot{y}_d = x_2 - \dot{y}_d. \quad (14)$$

Considering the TABLF as

$$V_1 = \frac{q_1(z_1)}{2p}\log\frac{k_{b_1}^{2p}(t)}{k_{b_1}^{2p}(t) - z_1^{2p}} + \frac{1-q_1(z_1)}{2p}\log\frac{k_{a_1}^{2p}(t)}{k_{a_1}^{2p}(t) - z_1^{2p}}, \quad (15)$$

where p is a positive integer. $k_{a_1}(t)$, $k_{b_1}(t)$ are defined as

$$\begin{cases} k_{a_1}(t) = y_d(t) - k_{c_1}^l(t) \\ k_{b_1}(t) = k_{c_1}^u(t) - y_d(t) \end{cases} \quad (16)$$

where $k_{a_1}^l \le k_{a_1}(t) \le k_{a_1}^u$, $k_{b_1}^l \le k_{b_1}(t) \le k_{b_1}^u$, $k_{a_1}^l$, $k_{a_1}^u$, $k_{b_1}^l$, $k_{b_1}^u$ are constants.

$$\dot{V}_1 = \frac{q_1(z_1)\xi_{b_1}^{2p-1}}{k_{b_1}(t)(1-\xi_{b_1}^{2p})}\left[z_2 - (k_1 + k_1^u(t))z_1 + \Phi_1 - z_1\frac{\dot{k}_{b_1}(t)}{k_{b_1}(t)}\right] + \frac{1-q_1(z_1))\xi_{a_1}^{2p-1}}{k_{a_1}(t)(1-\xi_{a_1}^{2p})}\left[z_2 - (k_1 + k_1^u(t))z_1 + \Phi_1 - z_1\frac{\dot{k}_{a_1}(t)}{k_{a_1}(t)}\right]. \quad (21)$$

Note that $k_1^u(t) + q_1(z_1)(\dot{k}_{b_1}(t)/k_{b_1}(t)) + (1-q_1(z_1))(\dot{k}_{a_1}(t)/k_{a_1}(t)) \ge 0$, then it has

$$\dot{V}_1 \le \mu_1 z_1^{2p-1} z_2 - k_1\xi_1^{2p}/(1-\xi_1^{2p}) + \mu_1\Phi_1 z_1^{2p-1}. \quad (22)$$

According to Young's inequality

$$xy \le |x|^a/a + |y|^b/b, \quad (23)$$

where a>1, b>1, and (a-1)(b-1) = 1.

Then one can see that

$$\mu_1 z_1^{2p-1} z_2 \le \mu_1\left[(2p-1)z_1^{2p}/2p + z_2^{2p}/2p\right]. \quad (24)$$

Substituting (20) into (19), it yields

$$V_1 \le -k_1\xi_1^{2p}/(1-\xi_1^{2p}) - \tau_1 + \mu_1 z_2^{2p}/2p \quad (25)$$

where τ_1 is an adaptive parameter.

Step 2: The time derivative of z_2=x_2-α_1 is

$$\dot{z}_2 = \dot{x}_2 - \dot{\alpha}_1 = f_2(\bar{x}_2) + g_2(\bar{x}_3) - \dot{\alpha}_1. \quad (26)$$

Let

According to Eq. (11), the Eq. (15) can be rewritten as

$$V_1 = \left[log1/\left(1-\xi_1^{2p}\right)\right]/2p. \quad (17)$$

It is clear that the absolute value of ζ is less than 1. Thus, the V_1 is positive definite and continuously differentiable.

The time derivative of V_1 is

$$\dot{V}_1 = \frac{\xi_1^{2p-1}}{1-\xi_1^{2p}}\bullet\dot{\xi}_1 = \frac{q_1(z_1)\xi_{b_1}^{2p-1}}{k_{b_1}(t)(1-\xi_{b_1}^{2p})}\left[\dot{z}_1 - z_1\frac{\dot{k}_{b_1}(t)}{k_{b_1}(t)}\right] + \frac{1-q_1(z_1))\xi_{a_1}^{2p-1}}{k_{a_1}(t)(1-\xi_{a_1}^{2p})}\left[\dot{z}_1 - z_1\frac{\dot{k}_{a_1}(t)}{k_{a_1}(t)}\right]. \quad (18)$$

Introduce z_2=x_2-α_1 and choose the virtual controller α_1 as

$$\alpha_1 = -\left(k_1 + k_1^u(t)\right)z_1 + \dot{y}_d + \Phi_1 \quad (19)$$

where $k_1^u(t) = \sqrt{(\dot{k}_{b_1}(t)/k_{b_1}(t))^2 + (\dot{k}_{a_1}(t)/k_{a_1}(t))^2 + \beta_1}$, k_1 and β_1 are the positive design parameters, $\Phi_1 == -\lg(x_1)z_1$.

Substituting (19) into (14), it yields

$$\dot{z}_1 = z_2 - (k_1 + k_1^u(t))z_1 + \Phi_1. \quad (20)$$

Combine Eqs. (20) and (17) leads to

$$V_2 = V_1 + \left[\log1/(1-\xi_2^{2p})\right]/2p. \quad (27)$$

The time derivation of V_2 is given by

$$\dot{V}_2 = \dot{V}_1 + \xi_2^{2P-1}\dot{\xi}_2/(1-\xi_2^{2P}) = \dot{V}_1 + \frac{q_2(z_2)\xi_{b_2}^{2p-1}}{k_{b_2}(t)(1-\xi_{b_2}^{2p})}\left[\dot{z}_2 - z_2\frac{\dot{k}_{b_2}(t)}{k_{b_2}(t)}\right] + \frac{1-q_2(z_2))\xi_{a_2}^{2p-1}}{k_{a_2}(t)(1-\xi_{a_2}^{2p})}\left[\dot{z}_2 - z_2\frac{\dot{k}_{a_2}(t)}{k_{a_2}(t)}\right]. \quad (28)$$

The virtual control law α_2 is chosen as

$$\alpha_2 = \frac{1}{g_2(\bar{x}_2)}\times \left[\begin{array}{l} -\hat{\theta}^T\omega_2 - (k_2 + k_2^u(t))z_2 + \frac{\partial\alpha_1}{\partial x_1}x_2 + \Phi_2 \\ +\sum_{j=0}^{1}\frac{\partial\alpha_1}{\partial\zeta_1^{(j)}}\zeta_1^{(j+1)} + \frac{\partial\alpha_1}{\partial\hat{\theta}}\Gamma\tau_2 - \frac{\mu_1}{2p\mu_2}z_2 \end{array}\right] \quad (29)$$

where Γ is a design parameter, $\zeta_1=[y_d, k_{a_1}, k_{b_1}]$ and τ_2 is an adaptive parameter.

Let $z_3=x_3-\alpha_2$, and substituting (26) into (23), it yields

$$\dot{z}_2 = g_2(\bar{x}_2)z_3 - (k_2+k_2^u(t))z_2 - \tilde{\theta}^T\omega_2 + \Phi_2 + \\ + \partial\alpha_1/\partial\hat{\theta}(\Gamma\tau_2 - \dot{\hat{\theta}}) - \mu_1 z_2/2p\mu_2. \quad (30)$$

Substituting (30) into (28), it yields

$$\dot{V}_2 = \dot{V}_1 + h_1\begin{bmatrix} g_2(\bar{x}_2)z_2 - (k_2+k_2^u(t))z_2 - \tilde{\theta}^T\omega_2 + \Phi_2 \\ + \dfrac{\partial\alpha_1}{\partial\hat{\theta}}(\Gamma\tau_2 - \dot{\hat{\theta}}) - \dfrac{\mu_1 g_1(x_1)}{2p\mu_2} - z_2\dfrac{\dot{k}_{b_2}(t)}{k_{b_2}(t)} \end{bmatrix} + h_2\begin{bmatrix} g_2(\bar{x}_2)z_2 - (k_2+k_2^u(t))z_2 - \tilde{\theta}^T\omega_2 + \Phi_2 \\ + \dfrac{\partial\alpha_1}{\partial\hat{\theta}}(\Gamma\tau_2 - \dot{\hat{\theta}}) - \dfrac{\mu_1 g_1(x_1)}{2p\mu_2} - z_2\dfrac{\dot{k}_{a_2}(t)}{k_{a_2}(t)} \end{bmatrix}, \quad (31)$$

where $h_1 = \dfrac{q_2(z_2)\xi_{b_2}^{2p-1}}{k_{b_2}(t)(1-\xi_{b_2}^{2p})}$, $h_2 = \dfrac{(1-q_2(z_2))\xi_{a_2}^{2p-1}}{k_{a_2}(t)(1-\xi_{a_2}^{2p})}$.

Note that

$$k_2^u(t) + q_2(z_2)(\dot{k}_{b_2}(t)/k_{b_2}(t)) + \\ +(1-q_2(z_2))(\dot{k}_{a_2}(t)/k_{a_2}(t)) \geq 0,$$

then it has

$$\dot{V}_2 \leq V_1 + \mu_2 g_2(x_2)z_2^{2p-1}z_2 - \mu_2\tilde{\theta}^T\omega_2 z_2^{2p-1} - \\ - \frac{k_2\xi_2^{2p}}{1-\xi_2^{2p}} - \frac{\mu_1 g_1(x_1)z_2^{2p}}{2p} + \mu_2\Phi_2 z_2^{2p-1} + \\ + \mu_2\frac{\partial\alpha_1}{\partial\hat{\theta}}(\Gamma\tau_2 - \dot{\hat{\theta}})z_2^{2p-1}. \quad . \quad (32)$$

According to (23), the following inequality holds

$$\mu_2 g_2(\bar{x}_2)z_2^{2p-1}z_3 \leq \mu_2 g_2(\bar{x}_2)\begin{bmatrix}(2p-1)z_2^{2p}/2p + \\ + z_3^{2p}/2p\end{bmatrix}. \quad (33)$$

Substituting (17) and (24) into (23), the derivative V_2 is given by

$$\dot{V}_2 = -\sum_{j=1}^{2}\frac{k_i\xi_i^{2p}}{1-\xi_i^{2p}} + \frac{1}{2p}\mu_2 g_2(\bar{x}_2)z_3^{2p} - \tilde{\theta}^T\tau_2 + \\ + \mu_2 z_2^{2p-1}\frac{\partial\alpha_1}{\partial\hat{\theta}}(\Gamma\tau_2 - \hat{\theta}). \quad (34)$$

Step 3: The controller is designed as

$$\mu = \alpha_n. \quad (35)$$

The adaptation law is designed as

$$\dot{\hat{\theta}} = \Gamma\tau_n. \quad (36)$$

The Lyapunov function is chosen as

$$V = V_2 + \left[\log 1/(1-\xi_3^{2p})\right]/2p + \tilde{\theta}^{T-1}\tilde{\theta}/2. \quad (37)$$

The time derivative of V is obtained by

$$\dot{V} \leq -\sum_{j=1}^{3}\frac{k_j\xi_j^{2p}}{1-\xi_j^{2p}} + \tilde{\theta}^T(\Gamma^{-1}\dot{\hat{\theta}})\tau_3 + \frac{\partial\alpha_1}{\partial\hat{\theta}}\mu_2 z_2^{2p-1} + \\ + (\Gamma\tau_j - \dot{\hat{\theta}}) + \frac{\partial\alpha_1}{\partial\hat{\theta}}\Gamma\mu_2 z_2^{2p-1}\mu_2\omega_2 z_2^{2p-1}. \quad (38)$$

Then, one can see that

$$\dot{V} \leq -\sum_{j=1}^{3}\frac{k_j\xi_j^{2p}}{1-\xi_j^{2p}}. \quad (39)$$

Hence, if the state initial values satisfy $k_{c_i}^l(0) < x_i(0) < k_{c_i}^u(0)$, then the error signals are bounded by $-D_{z_i}^l(t) < z_i(t) < D_{z_i}^u(t)$. In addition, the asymmetric time-varying state constraints are never violated, $k_{c_i}^l(t) < x_i(t) < k_{c_i}^u$, $\forall t > 0$. From the above descriptions, we can know that all the signals in the closed-loop are bounded.

4. Comparative simulation studies

To verify the effectiveness of the proposed control scheme, PID and AC are compared in simulation. The simulation parameters of hydraulic servo system are listed in Table 1. For evaluating the tracking performance of the compared controllers, the maximum Me, average μ, and standard deviation σ of the tracking errors are used to quantitatively assess the quality of different controllers. The performance indices are defined as follows.

$$\begin{cases} M_e = \max\limits_{i=1,\cdots N}|e_1(i)| \\ \mu = \dfrac{1}{N}\sum\limits_{i=1}^{N}|e_1(i)| \\ \sigma = \sqrt{\dfrac{1}{N}\sum\limits_{i=1}^{N}\left[|e_1(i)| - \mu\right]^2} \end{cases}. \quad (40)$$

The controller parameters of three different controllers are selected by multiple debugging. More importantly, all the control strategies operate under their optimal parameters to guarantee that the results are convincing.

1. BLBAC: The controller parameters are selected as k_1=2, k_2=3, β_1=5, β_2=7, p=2, and Γ=*dig*(3, 2).

2. AC: The control law is given by:

$u = -\hat{a}_0 y - \hat{a}_1\dot{y} - a_2\ddot{y} + \dot{\alpha}_2 - k_{01}e_3$, $\alpha_2 = -k_{02}\dot{x} - \alpha_1 + \dot{\alpha}_1 - e_2$,

Table 1
Simulation parameters of hydraulic servo system

Parameter	Value
m	200 kg
V_t	7×10^{-5} m^3
ρ	890 kg/m^3
B	1000 N·s/m
C_t	5×10^{-3}
β_e	7×10^{8} Pa
K	8×10^{-7} m/V
A	3.12×10^{-4} m^2
P_s	4 MPa
k_v	3.12×10^{-4} m^2

$\alpha_1 = -k_{03}e_1 + \dot{y}$, $\alpha_0 = -k_{01}e_1$, $e_2 = \dot{y} - \alpha_1$ and $e_3 = \ddot{y} - \alpha_2$, k_{01}=2, k_{02}=3, k_{03}=3.

3. PID: As a classical control method, the gains of controller are tuned by intelligent optimization algorithm for obtain the good control performance, k_p=2, k_i=3, k_d=0.021.

The three controllers are first tested for a sinusoidal desired signal x_d=60sin(5πt), the trajectories of the proposed controller are diagrammed in Fig. 2, where $k_{c_1}^{l} = -60 + 40\sin(5\pi t)$, $k_{c_1}^{u} = 80 + 40\sin(5\pi t)$. It can be seen that state constraints are not breached. The adaption control law on the proposed controller is shown in Fig. 3, which verifies the estimation precision of the designed adaptive law.

The position tracking performance and corresponding tracking errors of the sinusoidal signal are given in Fig. 4-5. It is noted that the proposed BLBAC can achieve satisfactory control performance. In these three controllers, PID produces the worst control performance. Without using barrier Lyapunov, the tracking performance of AC is worse than BLBAC, which validate the anti-interference ability of BLBAC. The performance indices of sinusoidal signal are collected in Table 2. It is seen that compared with PID (M_e= 5.9463 mm, μ=3.1881 mm, σ=1.5330 mm) and AC (M_e= 4.6490 mm, μ=2.3758 mm, σ=11.1622 mm), the proposed BLBAC (M_e= 3.6420 mm, μ=1.2018 mm, σ=0.6657 mm) achieve the smaller tracking error in both transient and state-steady performance. This is because the barrier-Lyapunov function is introduced in controller design

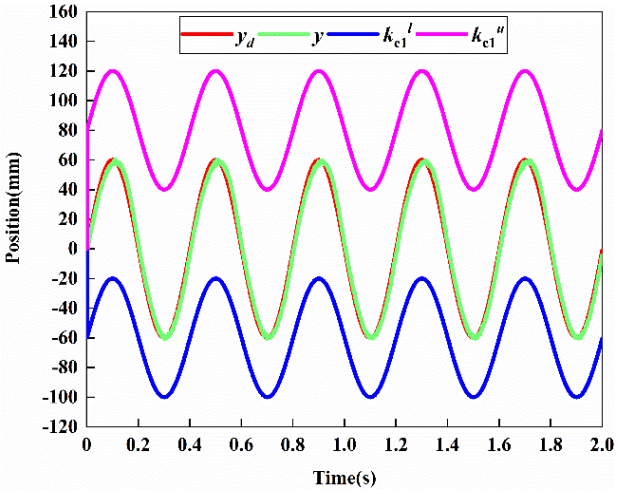

Fig. 2 Trajectories of y_d, y, $k_{c_1}^{l}$ and $k_{c_1}^{u}$

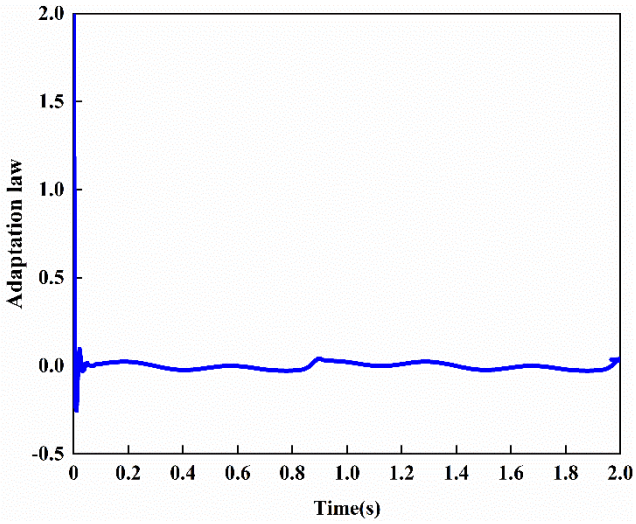

Fig. 3 Trajectory of adaptation law

to prevent the constraints overstepped. Contrastive control inputs of PID, AC, BLBAC are shown in Fig. 6, which are continuous and bounded. It is worth noting that the control input of BLBAC is smaller than that of PID and AC, which is owing to that BLBAC has better tracking performance than PID and AC control methods.

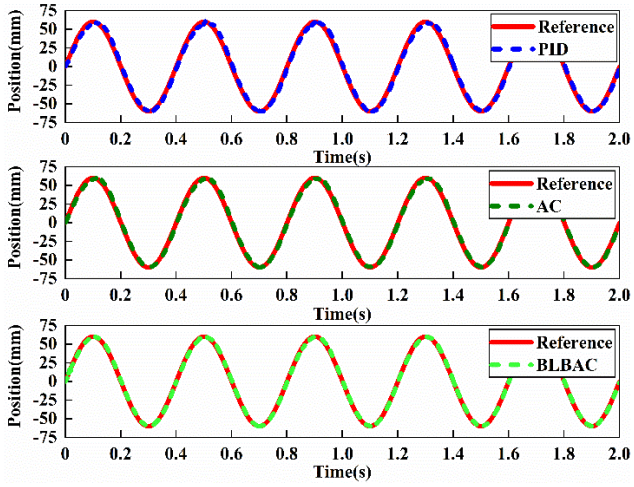

Fig. 4 Position tracking performance of sinusoidal signal

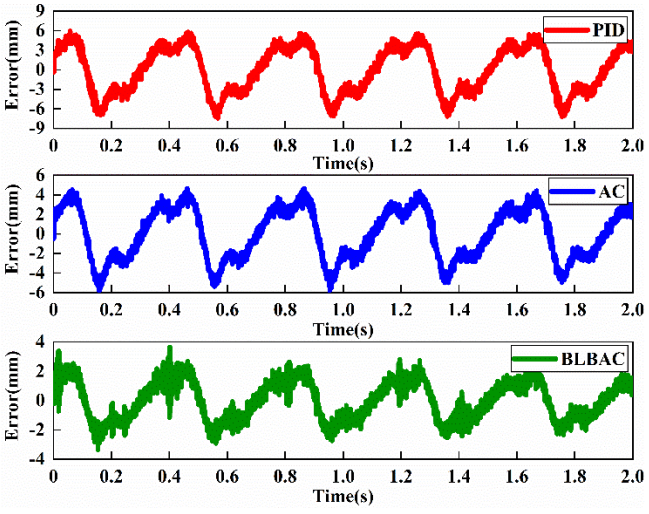

Fig. 5 Position tracking error of sinusoidal signal

Table 2
Performance indices of sinusoidal signal

Indices	M_e	μ	σ
PID	5.9463	3.1881	1.5330
AC	4.6490	2.3758	1.1622
BLBAC	3.6420	1.2018	0.6657

To further validate the performance of the proposed controller, a multi-frequency desired reference signal x_d=50sin(5πt)+40sin(10πt)+20sin(25πt) is applied. The comparative position tracking and corresponding tracking error of three controllers are shown in Figs. 7 and 8. The simulation results indicate that the proposed BLBAC controller obtain the best tracking performance among three controllers. It demonstrates the superiority of the proposed control scheme in dealing with t parametrical nonlinearities and model uncertainties encountered by the hydraulic servo system.

And the performance indices of multi-frequency sinusoidal signal are collected in Table 3. It is obvious that the proposed BLBAC controller obtains the tracking performance in terms of three performance indices, i.e, M_e= 7.4530 mm, μ=1.5223 mm, σ=1.6674 mm by the proposed controller, M_e= 10.3410 mm, μ=2.1917 mm, σ=2.2614 mm by AC controller, M_e= 16.4560 mm, μ=5.5832 mm, σ=3.3801 mm by PID controller. The

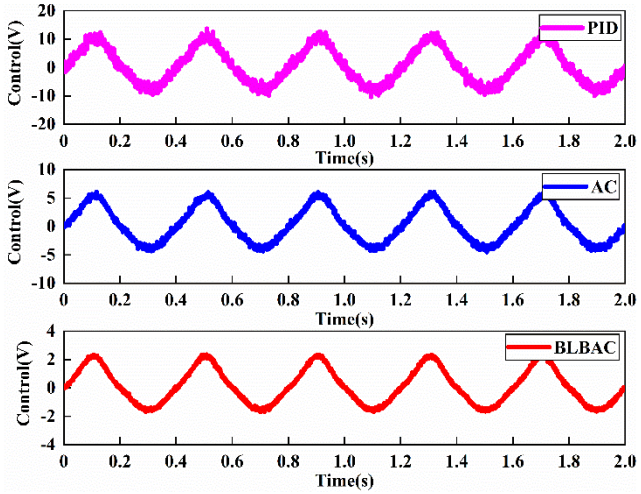

Fig. 6 Control input of sinusoidal signal

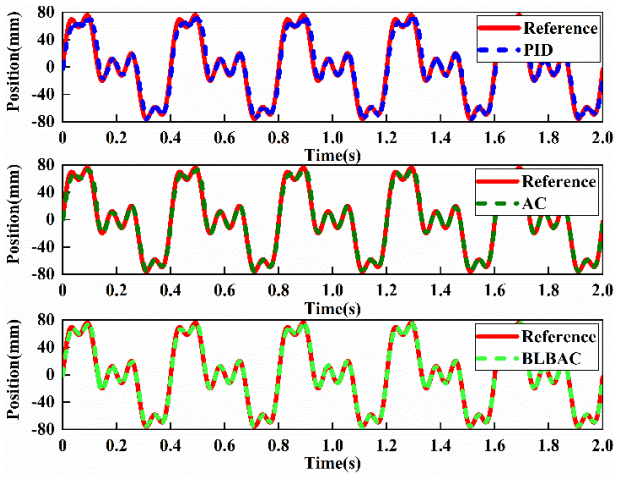

Fig. 7 Position tracking performance of multi-frequency sinusoidal signal

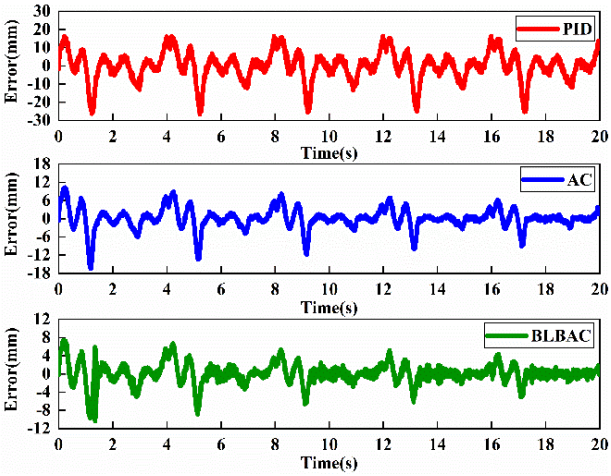

Fig. 8 Position tracking error of multi-frequency sinusoidal signal

comparative control input results are given in Fig. 9. One can find in Fig.9 that although the control inputs of three controllers are bounded, the BLBAC provides smoother control signal and generates less fluctuation compared to the other two controllers.

Table 3
Performance indices of multi-frequency sinusoidal signal

Indices	M_e	μ	σ
PID	16.4590	5.5832	5.3801
AC	10.3410	2.1917	2.6114
BLBAC	7.4530	1.5223	1.6674

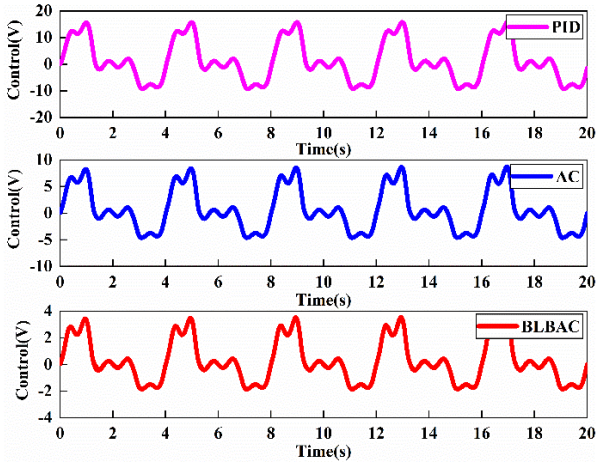

Fig. 9 Control input of multi-frequency sinusoidal signal

5. Conclusion

In this paper, an adaptive controller based on Barrier-Lyapunov has been proposed for trajectory tracking control of hydraulic servo systems in the presence of parametric uncertainties, unmodeled dynamics and external disturbances. To improve the position tracking performance, the dynamic model is first derived. To ensure the tracking trajectory and pressure within the boundaries of expectation, the time varying Barrier-Lyapunov is employed, which guarantees the tracking error is asymptotic stable. Furthermore, a novel adaptive law is adopted to deal with the hydraulic parametric nonlinearities and modeling uncertainties. Comparative simulation results have proved the superiority of the proposed controller PLBAC over PID and AC.

Acknowledgments

The work is supported by the Science and Technology Key Project Foundation of Henan Provincial Education Department (Grant No. 23A460014) and the High Level Talent Foundation of Henan University of Technology (Grant No. 2020BS043).

References

1. **Guo, Q.; Chen, Z.; Shi, Y.; Li, X.; Yan, Y.; Guo, F.; Li, S.** 2022. Synchronous control for multiple electrohydraulic actuators with feedback linearization, Mechanical Systems and Signal Processing 178: 109280. https://doi.org/10.1016/j.ymssp.2022.109280.
2. **Yang, X.B.; Zheng, X.L.; Chen, Y.H.** 2018. Position Tracking Control Law for an Electro-Hydraulic Servo System Based on Backstepping and Extended Differentiator, IEEE-ASME Transactions on Mechatronics 23(1): 132-140. https://doi.org/10.1109/TMECH.2017.2746142.
3. **Hu, J.; Sha, Y.; Yao, J.** 2023. Dual neural networks based active fault-tolerant control for electromechanical systems with actuator and sensor failure, Mechanical Systems and Signal Processing 182: 109558. https://doi.org/10.1016/j.ymssp.2022.109558.
4. **Guo, K.; Li, M.; Shi, W.; Pan, Y.** 2022. Adaptive Tracking Control of Hydraulic Systems With Improved Parameter Convergence, IEEE Transactions on Industrial Electronics 69(7): 7140-7150. https://doi.org/10.1109/TIE.2021.3101006.
5. **Deng, W.; Yao, J.; Jiao, Z.; Liu, X.** 2022. High dynamic output feedback robust control of hydraulic flight motion simulator using a novel cascaded extended state observer, Chinese Journal of Aeronautics 35(7): 300-309. https://doi.org/10.1016/j.cja.2021.07.013.
6. **Shen, W.; Huang, H.L.; Wang, J.H.** 2019. Robust Backstepping Sliding Mode Controller Investigation for a Port Plate Position Servo System Based on an Extended States Observer, Asian Journal of Control 21(1): 302-311. https://doi.org/10.1002/asjc.1885.
7. **Kim, W.; Won, D.; Shin, D.; Chung, C.C.** 2012. Output feedback nonlinear control for electro-hydraulic systems, Mechatronics 22(6): 766-777. https://doi.org/10.1016/j.mechatronics.2012.03.008.
8. **Yin, L.; Yang, X.; Deng, W.; Yao, J.** 2022. Super-twisting estimator based velocity-free robust tracking control of electro-hydraulic actuators, International Journal of Adaptive Control and Signal Processing 37(2): 538-552. https://doi.org/10.1002/acs.3536.
9. **Razzaghian, A.; Moghaddam, R.K.; Pariz, N.** 2021. Fractional-order nonsingular terminal sliding mode control via a disturbance observer for a class of nonlinear systems with mismatched disturbances, Journal of Vibration and Control 27(1-2): 140-151. https://doi.org/10.1177/1077546320925263.
10. **Na, J.; Li, Y.P.; Huang, Y.B.; Gao, G.B.; Chen, Q.** 2020. Output Feedback Control of Uncertain Hydraulic Servo Systems, IEEE Transactions on Industrial Electronics 67(1): 490-500. https://doi.org/10.1109/TIE.2019.2897545.
11. **Jing, C.H.; Xu, H.G.; Jiang, J.H.** 2020. Practical torque tracking control of electro-hydraulic load simulator using singular perturbation theory, ISA Transactions 102: 304-313. https://doi.org/10.1016/j.isatra.2020.02.035.
12. **Wang, S.B.; Na, J.; Xing, Y.S.** 2021. Adaptive Optimal Parameter Estimation and Control of Servo Mechanisms: Theory and Experiments, IEEE Transactions on Industrial Electronics 68(1): 598-608. https://doi.org/10.1109/TIE.2019.2962445.
13. **Shao, K.; Zheng, J.C.; Huang, K.; Wang, H.; Man, Z.H.; Fu, M.Y.** 2020. Finite-Time Control of a Linear Motor Positioner Using Adaptive Recursive Terminal Sliding Mode, IEEE Transactions on Industrial Electronics 67(8): 6659-6668. https://doi.org/10.1109/TIE.2019.2937062.
14. **Yang, M.X.; Zhang, Q.; Lu, X.L.; Xi, R.R.; Wang, X.S.** 2019. Adaptive Sliding Mode Control of a Nonlinear Electro-Hydraulic Servo System for Position Tracking, Mechanika 25(4): 283-290. https://doi.org/10.5755/j01.mech.25.4.22822.
15. **Zhao, J.; Na, J.; Gao, G.B.** 2022. Robust tracking control of uncertain nonlinear systems with adaptive dynamic programming, Neurocomputing 471: 21-30. https://doi.org/10.1016/j.neucom.2021.10.081.
16. **Cheng, C.; Liu, S.Y.; Wu, H.Z.** 2020. Sliding mode observer-based fractional-order proportional-integral-derivative sliding mode control for electro-hydraulic servo systems, Proceedings of the Institution of Mechanical Engineers Part C-Journal of Mechanical Engineering Science 234(10): 1887-1898. https://doi.org/10.1177/0954406220903337.
17. **Palli, G.; Strano, S.; Terzo, M.** 2018. Sliding-mode observers for state and disturbance estimation in electro-hydraulic systems, Control Engineering Practice 74: 58-70. https://doi.org/10.1016/j.conengprac.2018.02.007.
18. **Guo, Q.; Zhang, Y.; Celler, B.G.; Su, S.W.** 2016. Backstepping Control of Electro-Hydraulic System Based on Extended-State-Observer With Plant Dynamics Largely Unknown, IEEE Transactions on Industrial Electronics 63(11): 6909-6920. https://doi.org/10.1109/TIE.2016.2585080.
19. **Liu, W.; Lim, C.-C.; Shi, P.; Xu, S.** 2017. Backstepping Fuzzy Adaptive Control for a Class of Quantized Nonlinear Systems, IEEE Transactions on Fuzzy Systems 25(5): 1090-1101. https://doi.org/10.1109/TFUZZ.2016.2598360.
20. **Zhuang, H.X.; Sun, Q.L.; Chen, Z.Q.; Jiang, Y.X.** 2020. Back-stepping sliding mode control for pressure regulation of oxygen mask based on an extended state observer, Automatica 119: 109106. https://doi.org/10.1016/j.automatica.2020.109106.
21. **Shen, W.; Wang, J.H.; Huang, H.L.; He, J.Y.** 2019. Fuzzy sliding mode control with state estimation for velocity control system of hydraulic cylinder using a new hydraulic transformer, European Journal of Control 48: 104-114. https://doi.org/10.1016/j.ejcon.2018.11.005.
22. **Yang, G.; Yao, J.; Dong, Z.** 2022. Neuroadaptive learning algorithm for constrained nonlinear systems with disturbance rejection, International Journal of Robust and Nonlinear Control 32(10): 6127-6147.

https://doi.org/10.1002/rnc.6143.
23. **Chen, Z.; Huang, F.H.; Sun, W.C.; Gu, J.; Yao, B.** 2020. RBF-Neural-Network-Based Adaptive Robust Control for Nonlinear Bilateral Teleoperation Manipulators With Uncertainty and Time Delay, IEEE-ASME Transactions on Mechatronics 25(2): 906-918. https://doi.org/10.1109/TMECH.2019.2962081.
24. **Yao, J.Y.** 2018. Model-based nonlinear control of hydraulic servo systems: Challenges, developments and perspectives, Frontiers of Mechanical Engineering 13(2): 179-210. https://doi.org/10.1007/s11465-018-0464-3.
25. **Yao, J.Y.; Deng, W.X.; Jiao, Z.X.** 2015. Adaptive Control of Hydraulic Actuators With LuGre Model-Based Friction Compensation, IEEE Transactions on Industrial Electronics 62(10): 6469-6477. https://doi.org/10.1109/TIE.2015.2423660.
26. **Chen, X.; Deng, W.; Yao, J.; Liang, X.; Zhang, Z.** 2021. Robust indirect adaptive control of electromechanical servo systems with uncertain time-varying parameters, International Journal of Control 96(4): 869-882. https://doi.org/10.1080/00207179.2021.2016978.
27. **Guo, Q.Y.; Shi, G.L.; Wang, D.M.; He, C.Y.** 2017. Neural network-based adaptive composite dynamic surface control for electro-hydraulic system with very low velocity, Proceedings of the Institution of Mechanical Engineers Part I-Journal of Systems and Control Engineering 231(10), 867-880. https://doi.org/10.1177/0959651817731976.
28. **Liu, Y.-J.; Tong, S.** 2016. Barrier Lyapunov Functions-based adaptive control for a class of nonlinear pure-feedback systems with full state constraints, Automatica 64: 70-75. https://doi.org/10.1016/j.automatica.2015.10.034.
29. **Song, Y.; Xia, Y.; Wang, J.; Li, J.; Wang, C.; Han, Y.; Xiao, K.** 2022. Barrier Lyapunov function-based adaptive prescribed performance control of the PMSM used in robots with full-state and input constraints, Journal of Vibration and Control 29(5-6):1400-1416. https://doi.org/10.1177/10775463211063256.
30. **Liu, Y.-J.; Tong, S.** 2017. Barrier Lyapunov functions for Nussbaum gain adaptive control of full state constrained nonlinear systems, Automatica 76: 143-152. https://doi.org/10.1016/j.automatica.2016.10.011.

Z. Wan, Y. Fu, C. Liu, L. Yue

BARRIER LYAPUNOV BASED ADAPTIVE CONTROL FOR HYDRAULIC SERVO SYSTEMS WITH PARAMETRICAL NONLINEARITIES AND MODELING UNCERTAINTIES

S u m m a r y

Load variations, friction, and external disturbance degrade the control performance of hydraulic servo systems. To attain the high precision trajectory tracking performance for the hydraulic servo systems, a barrier Lyapunov based adaptive controller (BLBAC) is proposed in this paper. For the controller, the adaptive law is developed in each step of backstepping design such that the tracking error can converge to a prescribed accuracy. The state-constrained control of hydraulic servo systems is another issue worthy of attention. Hence, a novel time-varying asymmetric barrier Lyapunov function (TABLF) are adopted to guarantee that the states are not to violate their constraints. The closed-loop signals stability is proved by Lyapunov theory. Comparative simulation results verify the effectiveness of the proposed controller in comparison with the other two controllers for hydraulic servo systems.

Keywords: adaptive control, hydraulic servo systems, nonlinearities, uncertainties, Barrier-Lyapunov function.

Received January 28, 2024
Accepted August 19, 2024